CORROSION SCIENCE AND TECHNOLOGY, Vol.31, No.4(2002), pp.335~342

Accelerated Corrosion Induced by Chlorides in Simulated Waste Incineration Environment of Several Engineering Materials and Pure Metals

Y. S. Li, Y. Niu, and W. T. Wu

State Key Laboratory for Corrosion and Protection, Institute of Metal Research
The Chinese Academy of Sciences, Shenyang 110016 China

Corrosion problems in many industrial environments, such as waste incinerators or other advanced combustion power generation systems, are usually rather severe due to ash deposits of heavy and/or alkali metal chlorides and sulfate salts, especially those of Zn, K, Pb etc. In the present study, the individual effect of $ZnCl_2$ and KCl on the corrosion behavior of pure metals such as Fe, Ni, Cr and Al, several Ni- and Fe-based alloys as well as Fe-Al intermetallics, was examined at 450℃ in oxidizing atmosphere. On the other hand, the corrosion tests of one carbon steel and 310SS with and without aluminide coatings were also conducted beneath thin KCl salt films at 650℃, to study whether aluminide coating is a suitable protective means against such corrosives. As a conclusion, most of the materials suffered from accelerated corrosion beneath KCl, $ZnCl_2$, and $ZnCl_2$-KCl mixture deposits, characterized by rapid formation of porous, multi-layered and protective-less oxide scales as well as localized corrosion induced by chlorine. The oxide scales formed on pure Fe and pure Ni were rather thick and porous, while the most serious spallation of the corrosion products occurred on pure Cr. Ni-based alloys exhibited comparatively lower corrosion rates than Fe-based alloys, and Al either as bulk alloying element or as overlay coatings could remarkably enhance corrosion resistance of the alloys due to formation of a protective external alumina-rich scale. Finally, continuous mass loss was observed for Fe-based alloys during immersion test in $ZnCl_2$-KCl molten salts, and the corrosion was depressed with increasing Cr or Ni content, which was quite different from the results obtained in the case with salt deposits, as a direct consequence of the insufficient oxygen supply in the molten salts.

Keywords : *Fe-based alloy, Ni-based alloy, aluminized coating, chloride, corrosion*

1. Introduction

Recently incineration has been adopted as an effective and hygienic means for disposal of the ever-increasing voluminous industrial and municipal solid waste in many countries. For example, in Western Europe only, about 600 plants are in operation and the number is still increasing. Even though it is still a new business in China, many big cities such as Shanghai, Beijing, Shenyang etc, are planning from now on, to build more large-scale waste incineration plants in the near future, encouraged by the fact that the average heat of combustion of municipal waste in China has increased greatly and may reach 4180KJ/kg or above, which is very suitable for incineration disposal.[1)]

In most cases, the corrosion problem in incineration environments is very severe due to heavy corrosiveness of the combustion gases containing HCl/Cl_2 or SO_2 and salt deposits ($ZnCl_2$, KCl, NaCl, Na_2SO_4, etc) with low melting point, and thereby, metallic materials usually undergo degradation in service. For example, the superheater tube materials used in the waste incinerator in Shenzhen city degraded seriously in less than three months after service, and had to be changed totally. However, more attentions have been paid to the corrosion mechanisms caused by sulfate salts or gaseous chlorides up to now, yet the individual corrosion effect of the heavy metal (Sn, Pb, Zn) or alkali metal (K, Na) chlorides, which are actually the major components in deposits from waste incinerator, has not been examined thoroughly.[2-4)] In this study, the corrosion behavior of several Fe, Ni-based alloys as well as pure Fe, Cr, Ni, Al and Fe-Al intermetallics, is investigated in the presence of $ZnCl_2$ and/or KCl. For comparison, corrosion tests of one carbon steel and SS310 with aluminized coatings are also performed to examine the ability of coatings against such corrosive environments.

Table.1 Nominal chemical compositions of materials tested (in wt.%)

	Fe	Cr	Ni	Al	Other
Fe	bal.	–	–	–	–
Cr	–	bal.	–	–	–
Ni	–	–	bal.	–	–
Al	–	–	–	bal	–
2205	bal	22.20	5.80	–	Mn 1.56, Mo 3.05
Fe-10Cr	–	10	–	–	–
Fe-25Cr	–	25	–	–	–
Fe-Al	bal	–	–	28.5	–
M38G	–	16.34	bal	4.01	Co 8.38, Ti 3.81, Mo 1.77

2. Experimentals

The chemical compositions of the materials employed in this study are partially listed in Table 1, while two Al-rich coatings were prepared by conventional pack cementation process. The materials were machined into specimens with dimension of 10 x 15 x 1.5 mm, and then ground down to 600 SiC paper and subsequently cleaned with acetone. After being preheated, the samples then were pre-deposited either with KCl% of 1-2 mg/cm^2 or $ZnCl_2$-KCl (55: 45, molar fraction) mixture of 3-4 mg/cm^2 homogeneously on the surfaces by spraying the relevant salt saturated solutions.

The experiments were carried out in oxygen atmosphere with a flow velocity of 80ml/s controlled by capillary flowmeter, using a horizontal furnace with a quartz working tube. Each of the salt-deposited samples was hung in an alumina crucible with platinum wire; the crucibles were then placed into the horizontal furnace. The corrosion kinetics was measured regularly by moving out the samples and putting back after being weighed. Some typical samples were also corroded in molten salt for comparison purpose. After corrosion, the metallographical cross-sections were prepared by grinding in kerosene in order to prevent the dissolution of residual salts in the corrosion product. The morphology and composition examination was carried out using scanning electron microscopy (SEM), energy dispersive spectroscopy (EDX), and X-ray diffraction (XRD).

3. Results

3.1 Corrosion kinetics

Fig. 1a presents corrosion kinetic curves for several

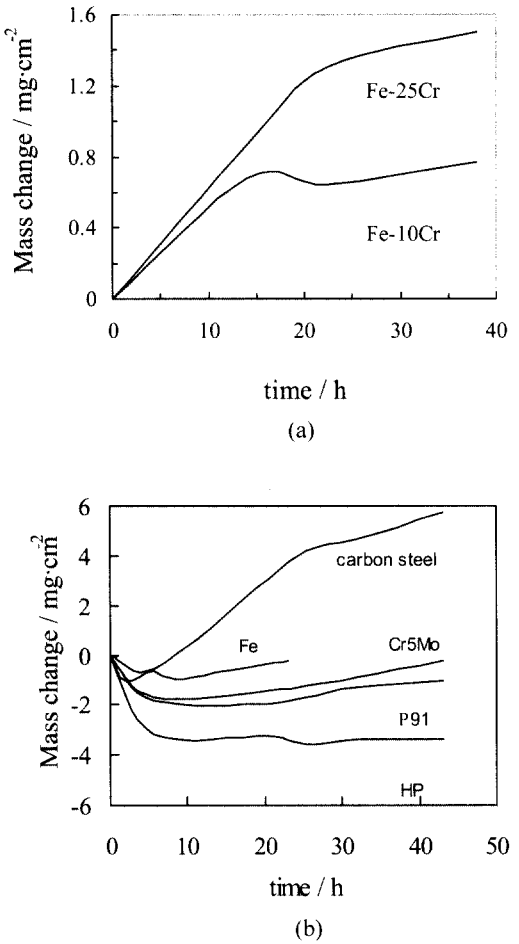

Fig. 1. Corrosion kinetics of examined materials beneath KCl (a) and $ZnCl_2$ (b) deposit at 450℃

materials beneath solid KCl deposit at 450℃. In fact, the mass change for aluminide coatings and Ni-based alloys was rather small and thus they are not showed in the fig. However, it can still be observed that the corrosion of Fe-Cr alloys was accelerated to some extent with increasing Cr content, quite different from that in merely oxidizing conditions. Fig. 1b provides the mass changes versus time for the corrosion beneath $ZnCl_2$ deposit; accelerated corrosion was still present within the whole corrosion duration. However, the mass changes were very irregular, and mass losses were always present during the initial corrosion stage, which may be due to the much stronger evaporation of $ZnCl_2$ salt than oxidant pickup at the initial period, and then gradually transited into the second stage of mass gain.

Fig. 2a shows the corrosion kinetic curves for the materials beneath $ZnCl_2$-KCl deposits at 450℃. Since the corrosion product on pure Cr spalled seriously during the initial corrosion stage (less than 1 h), its kinetic curve was not included in the diagram. It can be observed clearly

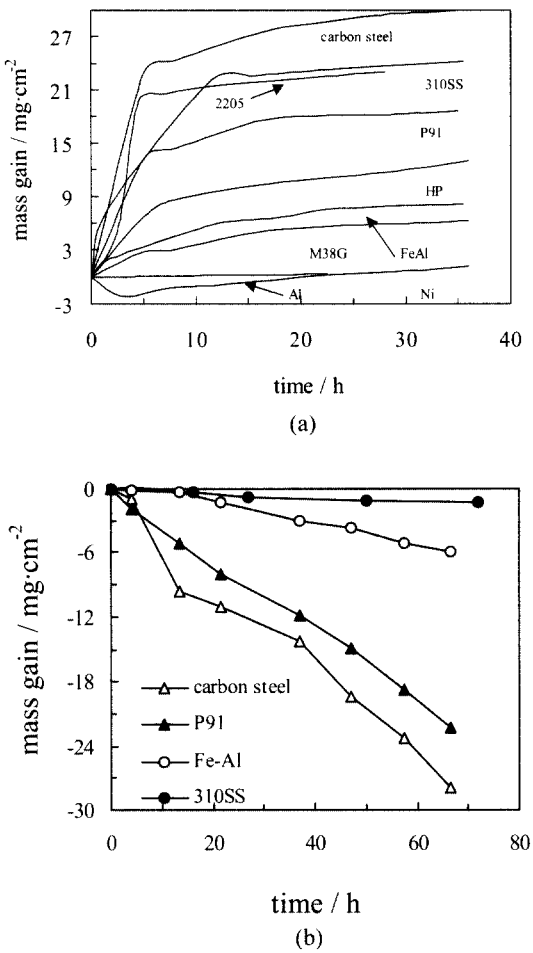

Fig. 2. Corrosion kinetics of examined materials beneath $ZnCl_2$-KCl deposit (a) and in molten $ZnCl_2$-KCl mixture by immersion test (b) at 450℃

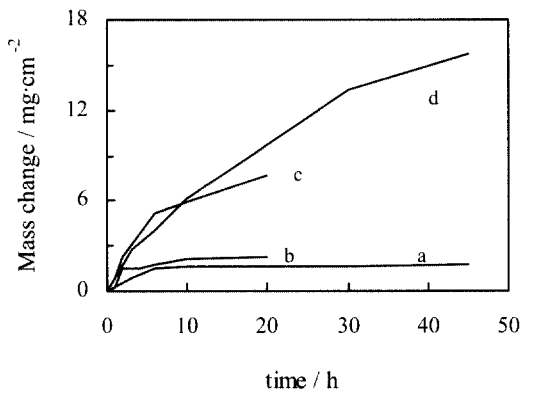

Fig. 3. Corrosion kinetics of carbon steel (a,d) and 310SS (b,c) with(a,b) or without (c,d) aluminized coating beneath KCl deposit at 650℃

that the corrosion rates were markedly enhanced at the initial stages, and then turned to the second stage with very slow rate. Among the materials, pure Fe and Fe-based alloys have higher mass gains, while increased Cr content did not suppress the corrosion rate of the alloys. On the contrary, pure Al, Ni suffered least attack, and Ni-based alloys and Fe-Al intermetallics also exhibit better corrosion resistance compared with heat-resistant alloys. Fig. 2b shows the mass-change kinetics for samples immersed in fused $ZnCl_2$-KCl mixture under 1 atm pure oxygen environment. The result differed a lot from that involving the $ZnCl_2$-KCl deposit, since corrosion resistance increased with increasing Cr content of alloys, and therefore, less mass change was observed for Ni-based alloys and high-Cr containing alloys. However, a premature melting like phenomenon occurs to pure Al under such situation. Fig. 3 shows the corrosion results for carbon steel and SS310 with and without Al-rich coating beneath KCl deposits at 650℃. It can be seen that corrosion resistance of the steels may also be improved significantly by aluminized coating.

3.2 Scale structure and composition

As typical examples, Fig. 4 presents the corrosion morphologies of pure Ni (a), and Fe-25Cr (b) after corrosion beneath KCl salt film. A thick yet very porous oxide scale formed on pure Ni, while the corrosion products on Fe-25Cr were rather complex, containing an external Fe oxide scale and an inner oxide layer rich in Cr. And the Cr content increased significantly from the external oxide scale to the scale/matrix interface, as shown by the EDX results.

For the materials corroded beneath $ZnCl_2$, Cl-rich corrosion products were frequently present either at the scale/substrate interface or in the matrix just beneath the scale, besides the formation of an external thick oxide scale, Fig. 5a. In the case of HP steel, which possesses austenitic matrix and Cr_7C_3 carbide as second phase, the carbides were preferentially attacked in comparison to the matrix and present as dark regions, as marked with an arrow in Fig. 5b.

The severest attack occurred for all the materials in case of $ZnCl_2$-KCl deposit. For example, the oxide scale formed on Fe was rather thick and exhibited distinctive detachments in the oxide scale, and porous NiO scale formed on pure Ni as external scale.[4] Compared with the results above, pure Al showed quite better corrosion resistance due to the presence of an alumina-rich external scale. In the case of pure Cr, however, the external Cr_2O_3 scale readily spalled during the initial corrosion stage, leaving powder-like corrosion products remained on the substrate surface.[4]

For the Fe-based alloys with higher Cr-content, multi-layered oxide scales formed rapidly during the initial

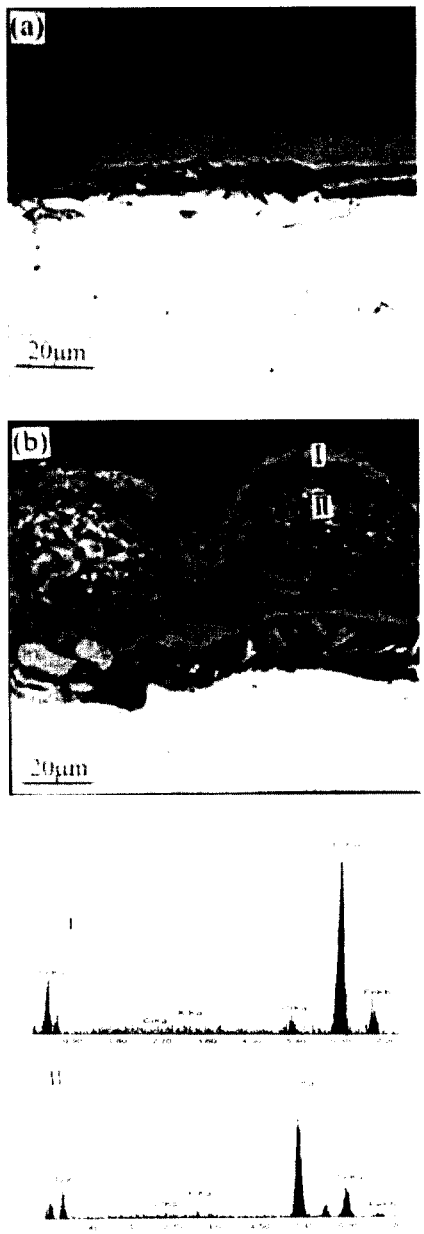

Fig. 4. Cross-sectional morphologies of pure Ni (a) and Fe-25Cr (b) corroded beneath KCl deposit at 450℃. (c): EDX results in (b)

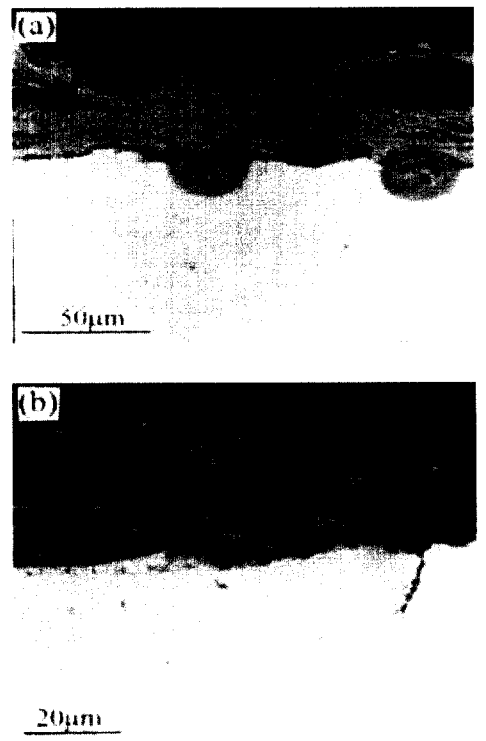

Fig. 5. Cross-sectional morphologies of carbon steel (a) and HP (b) corroded beneath $ZnCl_2$ deposit at 450℃

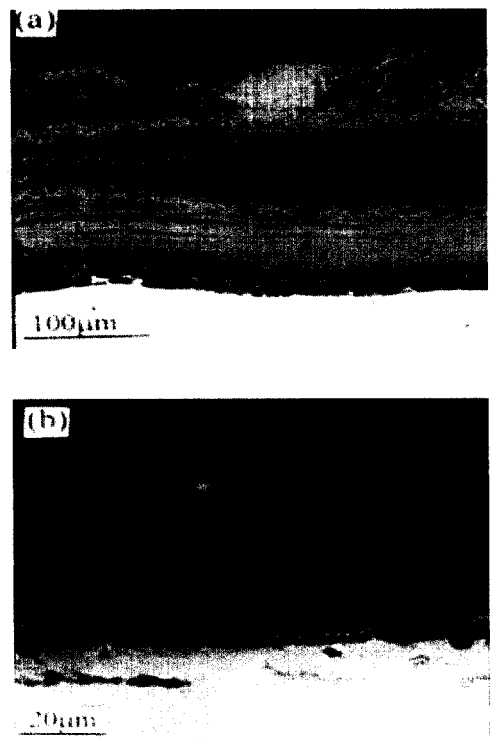

Fig. 6. Cross-sectional morphologies of Fe-25Cr (a) and M38G Ni-based alloy(b) corroded beneath $ZnCl_2$-KCl deposit at 450℃

period and spalled seriously thereafter (Fig. 6a). The compositions of the scales were very complex and inhomogeneous. In some cases, chlorine was enriched at the scale/substrate interface and even produced irregular local corrosion inside the matrix(grey-colored), either along the grain boundaries or Cr-rich carbides. Fig. 6b presents the microstructure of M38G, a Ni-based alloy. Nodules rich in Zn were observed on the sample surface, and the scale compositions were mainly composed of NiO with some Cr_2O_3. After corrosion beneath KCl salt film at 650℃,

both carbon steel and SS310 modified by aluminized coating formed an external alumina-rich scale and therefore corrosion resistance of the steels may be enhanced to some extent.

After corrosion in molten $ZnCl_2$-KCl salt by crucible tests, the precipitates on the surface of the salt on P91 steel contained 13 wt%O, 61 wt%Fe, 20 wt%Zn as well as small amount of Mg or Ca impurities, which might come from the crucible, while Cr content on the surface of the sample has increased to a higher degree.[4] For pure Al, after testing in molten $ZnCl_2$-KCl salt however, the corners and edges of the sample became round and thinner, whereas the two large surfaces swelled up as hill-like, which clearly implied that the sample experienced a premature melting during testing. It could be observed from the cross section of the sample (Fig. 7a-c) that there existed a rather thick periphery rich in zinc on the surface of the residual Al substrate. In fact, the Zn content of the periphery varied from 72wt% at the inner part near the Al matrix to 90wt% at the outer part of the light region, and it can be seen obviously that an Al-Zn eutectic has formed.

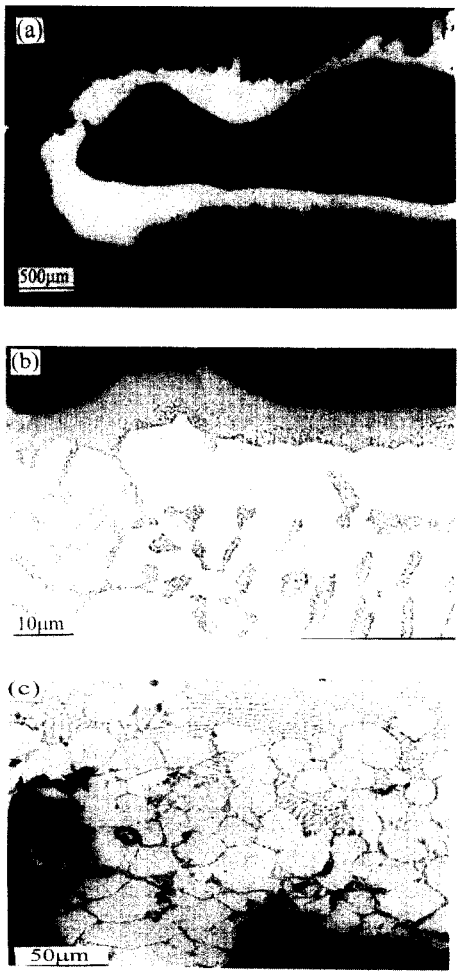

Fig. 7. Microstructures of pure Al corroded inside molten $ZnCl_2$-KCl salt at 450℃. (a): general view; (b): expanded view between the Al matrix(black) and the external area(light) interface; (c): expanded view of the outmost light region in (a)

4. Discussion

The oxidation rates of the tested materials are rather low at 450℃ in merely oxidizing environment without any chloride contamination. However, accelerated corrosion would occur once chlorides were present either as molten and in solid state or even as vapor phase. A surprising result in the present study is that the higher Cr content does not lead the alloys to from a compact scale effectively against such environment since the very poor adherence of the corrosion products to the matrix, which is quite different from the conventional hot corrosion behavior observed in the utility boilers and gas turbines where sulfate compounds are the main corrosive component. Similar examples can be found in many literatures.[5-9] Y. Shinata once examined the NaCl-induced hot-corrosion of SUS-304, SUS-316 and SUS-329J1 two-phase stainless steel,[5] and found that chromium was always oxidized selectively and formed a non-protective scale, therefore the corrosion loss increased with increasing Cr content. Especially in the two-phase stainless steel, the ferrite phase was even attacked more seriously than the austenitic phase because the ferrite has a higher Cr content. Zahs *et al*, studied the corrosion of Fe-Cr alloys in an HCl/N_2/He-5vol.%O_2 gas mixture, and observed that an increased Cr content did not lead to better corrosion resistance. On the contrary, both Fe-15Cr and Fe-35Cr were covered with a thick and porous scale, which had very poor adherence at the metal/scale interface and thereby easily spelled.[6] Wu *et al* recently examined the synergic effects of water vapor and NaCl solid deposit on the corrosion of pure Cr and Fe-Cr model alloys and revealed the detrimental role of Cr in such environment,[7,8] Further more, Fujikawa also reported the harmful influence of Cr on internal penetration attack for stainless steels at temperatures below the melting point of chloride.[9]

Thermodynamic consideration may be helpful to gain a better understanding about the effect of Cr in chlorine-containing environment, therefore a phase stability diagram of M-O-Cl system at 450℃ was built as shown in Fig. 8a, where M presents Fe, Cr and Ni at unit activity respectively. The comparative stability of oxides and chlorides depends mainly on the oxygen and chlorine partial pressures in the environment, and the oxygen partial pressure at the scale-matrix interface may be very low

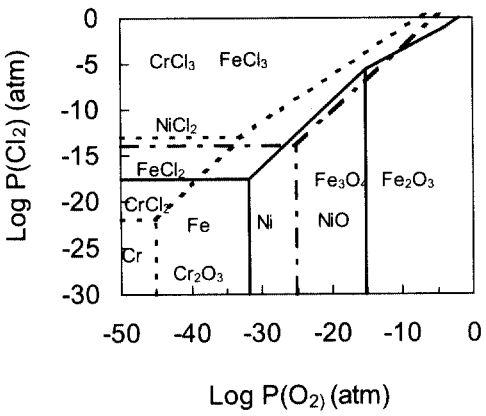

(a)

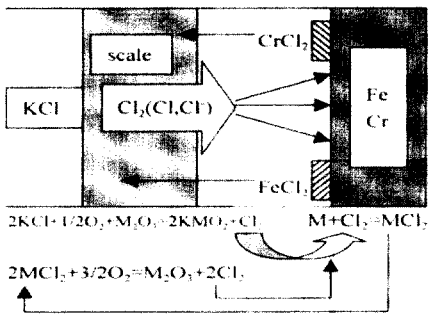

(b)

Fig. 8. Phase-stability diagram of M-O-Cl (a) at 450℃ and schematic diagram for the degradation mechanism beneath chloride salt film (b)

whereas the oxide is the most stable phase in the environment. However, the chlorine partial pressure may increase in this location of the scale-matrix interface to a large value and therewith the chloride will then become the most stable phase, instead of oxide. Since the vapor pressure of the chloride is usually far higher than that of the relevant oxide of the same metal, therefore, the volatile chlorides will diffuse or evaporate outwards and then convert into oxide particles again in the outer region of the oxide scale, which will produce significant growth stresses and cause the oxide scale to become less compact and poor protective. As a result, the transport of those reactant species will be accelerated. This process has been termed of "active oxidation",[10] and can also occur either in gaseous environment such as HCl, Cl_2 or metal chloride vapors as well as beneath solid salt films.

By comparing the characteristic differences concerning the corrosion behavior of the different metals, such as the free energy of chloride formation, the vapor pressure of the chloride and the oxygen pressure, by which conversion of the evaporated chloride into oxide may occur, it is found that higher reactivity is expected for Cr than for Fe and Ni, to form the correspondent divalent chlorides. On the other hand, Cr chloride can be converted into oxide at very low oxygen pressures, while chlorides of Fe and Ni always at significantly higher oxygen pressures.[11] Therefore the evaporating Cr chlorides are usually oxidized at the location much close to the matrix surface than that of Fe and Ni during their outward diffusion and, accordingly, more porosity and higher growth stresses arise. This may be an important reason for the worsen adherence of the oxide scales formed in high Cr-containing materials, as shown in the schema diagram describing the degradation mechanism (Fig. 8b).

As to the corrosion induced by $ZnCl_2$ or $ZnCl_2$-KCl, which become melt at certain temperature due to their low melting point, fluxing mechanism thus will be responsible for the more rapid degradation. In fact, assuming that a low oxygen partial pressure is established at the salt/matrix interface, Fe_2O_3 may dissolve into the salt forming soluble $FeCl_3$, according to the following reaction:

$$Fe_2O_3 + 6Cl^- = 2FeCl_3\ (diss.) + 3O^{2-} \quad (1)$$

The dissolved Fe chloride and the oxide-ions then diffuse outwards through the molten salt to the salt/gas interface, where Fe_2O_3 will precipitate due to higher PO_2:

$$2FeCl_3 + O^{2-} + O_2 = Fe_2O_3 + 3Cl_2 \quad (2)$$

The oxide scale formed by this way is rather porous and can hardly provide any effective protection. As a direct consequence, the corrosion will be significantly enhanced.

During the corrosion process, $ZnCl_2$ will be consumed rapidly due to its strong evaporability and reactivity, and accordingly the KCl content will enrich. Considering two facts i.e. the much higher corrosion rate occurred beneath mixed $ZnCl_2$-KCl than that for single $ZnCl_2$ salt, and the corrosion rate beneath pure KCl solid deposit at 450℃ is also much lower than those beneath mixed $ZnCl_2$-KCl (in molten salts), it may be expected that a new eutectic salt may be replenished. Takemura *etc*, once examined the chlorination-oxidation of low carbon steel in Cl_2-O_2 system with KCl deposit at 400℃, and noticed that if $FeCl_2$ was present in sufficient quantities, an eutectic salt solution of KCl and $FeCl_2$ could form with a melting point of 355℃, which could flux the protective oxide scale and produced accelerated corrosion. On the contrary, no obvious weight change was observed when either iron chlorine or KCl was absent in the corrosive environment.[12] In fact, some amount of potassium can be detected at the scale/matrix interface after short-time corrosion in this study, such as in SS310, it is reasonable to assume that a

liquid-salt solution of KCl-$FeCl_2$ formed, in which $FeCl_2$ may come either from the dissolution of Fe oxide into the chloride salt, or from the direct reaction between Fe and gaseous chlorine released by other reactions. This process was also discussed by Spiegel in detail,[3] with respect to the corrosion of pre-oxidized low alloying steel under similar conditions, but the oxygen pressure selected was much lower than the present study. In fact, KCl melt will readily react with the Fe oxide scale:

$$4KCl + 2Fe_2O_3 + O_2 = 2K_2Fe_2O_4 + 2Cl_2 \quad (3)$$

or

$$24KCl + 10Cr_2O_3 + 9O_2 = 12K_2CrO_4 + 8CrCl_3 \quad (4)$$

At the same time, reactions between KCl and the metal matrix may also occur once KCl penetrates onto the scale/metal interface through cracks or pores within the oxide scales:

$$2KCl + 2Fe + 2O_2 = K_2Fe_2O_4 + Cl_2 \quad (5)$$

$$6KCl + 8Fe + 6O_2 = 3K_2Fe_2O_4 + 2FeCl_3 \quad (6)$$

Therefore the corrosion rate will be accelerated due to the presence of the eutectic mixture.

Under the presence of molten chloride salt, the high Cr content in the materials was still unable to improve the corrosion resistance against the environment. In fact, solubility studies of the oxides in fused chloride salts can usually provide important information on the mode of dissolution of protective oxides, and some initial measurements have been carried out recently. For example, on assuming possible acid-base chemistry of fused chlorides, Ishitsuka *et* al.[13] measured the solubility of Cr_2O_3 in molten NaCl-KCl at 727°C in different levels of basicity, by introducing two parameters: i.e. HCl and H_2O, found that the Cr_2O_3 film easily dissolved in the molten chloride salt as hexavalent ion and thus lost its protective property:

$$2Cr_2O_3 + 3O_2 + 4O^{2-} = 4CrO_4^{2-} \quad (7)$$

A surprising result was present in Fig. 4, when corroded inside the fused chloride salts during crucible test, by which the corrosion resistance of those materials has increased with increasing Cr content, contrast sharply with that beneath $ZnCl_2$-KCl deposit. This difference most probably results from the insufficient oxygen supply. For example, according to the phase stability diagram for the Na-Cr-Cl-O system,[14] which showed that dissolution of protective Cr_2O_3 scale by acidic fluxing might result in the formation of highly volatile CrO_2Cl_2, a self-sustaining accelerated hot corrosion occurred for Cr_2O_3 forming

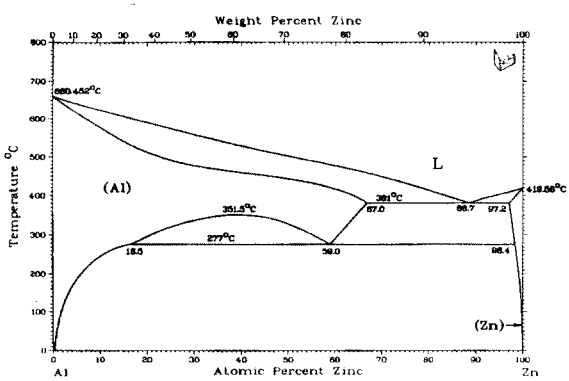

Fig. 9. Phase diagram of binary Al-Zn system

steels. Yet this acidic fluxing usually involves gaseous oxygen as a reactant, the reaction can be influenced seriously by the diffusion and solubility of oxygen in the melt. As a direct consequence, once the diffusion of oxygen in the melt is rate-limiting factor, fluxing will be suppressed in contrast with other oxides such as Fe_2O_3 and NiO. In the case of the corrosion beneath salt deposit, since the layer of deposits was so thin as little effective barrier for oxygen and oxide scales were rather porous and can hardly provide any effective protection, the corresponding oxygen supply would be more sufficient than that for immersed in molten salts, and severer attack was therefore reasonably expected.

The chlorine attack also resulted in extreme internal penetration attack as well as general corrosion. For example, a preferential attack of Cr_7C_3 carbides was present in HP steel, and the reaction can be described as:

$$2Cr_7C_3 + 14Cl_2 + 3O_2 = 14CrCl_2 + 6CO \quad (8)$$

In fact, fully over-sensitized steels tend to suffer from much severer inter-granular attack than solution-treated steels due to the preferential attack of Cr carbides by chlorine. Therefore, Cr may exhibit harmful influence with respect to the internal penetration attack.

As to the rapid dissolution of Al in molten ZnCl-KCl salt, a replacement reaction may be responsible for the result, just as a direct consequence of the more reactive thermodynamic stability chloride of Al than that of Zn:

$$Al + ZnCl_2 = AlCl_3 + Zn \quad (9)$$

The highly volatile $AlCl_3$ will be released into the environment while Zn deposits on the surface of Al matrix, which according to the Al-Zn phase diagram will lead to the formation of low melting point of Al-Zn alloy[15] (Fig. 9). Finally, Fe-Al intermetallics and Al-rich coatings showed quite low corrosion rate in the same environment compared with those Fe-based alloys, which was most

probably due to the formation of an Al_2O_3-rich external scale. In fact, since aluminum chloride ($AlCl_3$) has much higher vapor pressure than those chlorides such as Fe, Ni and Cr, it will diffuse outwards more readily and reach the outmost of the scale, where the conversion from chloride to oxide will occur since this only needs a very low oxygen partial pressure. However, more work is required in the future to evaluate its protective property since the mechanism is still not well understood at present due to the complexity of the system examined.

5. Conclusions

1) All the tested materials suffered from accelerated corrosion with the presence of chloride deposits in oxidizing environment, and non-protective oxide scales formed as well as local corrosion inside the matrix induced by chlorine.

2) The adherence of the corrosion products to the substrate generally worsen with increasing Cr content for Fe-based alloys, while the corrosion resistance could be improved to some degree with increasing Ni content.

3) Iron aluminide and aluminized coating on steels all exhibited comparatively better corrosion resistance to chloride deposits due to the formation of an external alumina-rich scale, whereas the reaction mechanism still needs further illustration.

Acknowledgements

Financial support by the National Natural Science Foundation of China is gratefully acknowledged.

References

1. Y. S. Li, Y. Niu, W. T. Wu, *Corrosion Science and Protection Technology.*, **12**, 224 (2000).
2. E. Otero, A. Pardo, F. J. Perez, M. V. Utrilla, and T. Levi, *Oxid. Met.*, **49**, 467 (1998).
3. M. Spiegel, *Mater. Corros.*, **373**, 50 (1999).
4. Y. S. Li, Y. Niu, and W. T. Wu, CORRORION/2001, Paper No. 01158. (Houston, TX: NACE International), (2001).
5. Y. Shinata, F. Takahashi, and K. Hashiura, *Mater. Sci. Eng.*, **87**, 399 (1987).
6. A. Zahs, M. Spiegel, and H. J. Grabke, *Mater. Corros.*, **50**, 561 (1999).
7. Weitao Wu, Fuhui Wang, and Yonghua Shu, in HIGH TEMPERATURE CORROSION AND PROTECTION 2000, edited by T.Narita, T.Maruyama and S.Taniguchi, The proceedings of the International Symposium on High-Temperature Corrosion and Protection 2000, Science Reviews, Sept. 239-246 (2000).
8. Y. H. Shu, F. H. Wang, and W. T. Wu, *Oxid. Met.*, **51**, 97 (1999).
9. H. Fujikawa and N. Maruyama. *Mater. Sci. Eng.*, **A120**, 301 (1989).
10. Y. Y. Lee and M. J. McNallan, *Metal. Trans.*, **18A**, 1099 (1987).
11. A. Zahs, M. Spiegel, and H.J. Grabke, *Corros. Sci.*, **42**, 1093 (2000).
12. M. Takemura and M.J. McNallan, CORROSION/95, paper No. 568, (Houston, TX: NACE International), (1995).
13. T. Ishitsuka and K. Nose, *Mater. Corrosion.*, **177**, 51 (2000).
14. N. Otsuka and T. Kudo, in High temperature corrosion of advanced materials and protective coatings, Y. Saito, B. Onay and T. Maruyama(Eds.), North Holland, Elsevier Science Publishers, 205 (1992).
15. T. B. Massalski, Binary Alloys Phase Diagram, ASM, USA, 185 (1990).